Human Molecular Genetics, 2011, Vol. 20, No. 1 **165–175**
doi:10.1093/hmg/ddq455
Advance Access published on October 11, 2010

Protein kinase A regulates caspase-1 via Ets-1 in bone stromal cell-derived lesions: a link between cyclic AMP and pro-inflammatory pathways in osteoblast progenitors

Madson Q. Almeida[1], Kit Man Tsang[1], Chris Cheadle[5], Tonya Watkins[5], Jean-Charles Grivel[3], Maria Nesterova[1], Raphaela Goldbach-Mansky[4] and Constantine A. Stratakis[1,2,*]

[1]Section on Endocrinology and Genetics, Program on Developmental Endocrinology and Genetics (PDEGEN), [2]Pediatric Endocrinology Inter-Institute Training Program, *Eunice Kennedy Shriver* National Institute of Child Health and Human Development (NICHD), [3]Program on Physical Biology, NICHD and [4]Translational Autoinflammatory Disease Section, NIAMS, National Institutes of Health (NIH), Bethesda, MD 20892, USA and [5]Genomics Core, Division of Allergy and Clinical Immunology, School of Medicine, Johns Hopkins University, Mason Lord Building, Center Tower, Room 664, 5200 Eastern Avenue, Baltimore, MD 21224, USA

Received September 10, 2010; Revised September 10, 2010; Accepted October 6, 2010

Patients with genetic defects of the cyclic (c) adenosine-monophosphate (AMP)-signaling pathway and those with neonatal-onset multisystem inflammatory disease (NOMID) develop tumor-like lesions of the long bones. The molecular basis of this similarity is unknown. NOMID is caused by inappropriate caspase-1 activity, which in turn activates the inflammasome. The present study demonstrates that NOMID bone lesions are derived from the same osteoblast progenitor cells that form fibroblastoid tumors in mice and humans with defects that lead to increased cAMP-dependent protein kinase A (PKA) signaling. NOMID tumor cells showed high PKA activity, and an increase in their cAMP signaling led to PKA-specific activation of caspase-1. Increased PKA led to inflammation-independent activation of caspase-1 via over-expression of the proto-oncogene (and early osteoblast factor) Ets-1. In NOMID tumor cells, as in cells with defective PKA regulation, increased prostaglandin E2 (PGE2) led to increased cAMP levels and activation of Wnt signaling, like in other states of inappropriate PKA activity. Caspase-1 and PGE2 inhibition led to a decrease in cell proliferation of both NOMID and cells with abnormal PKA. These data reveal a previously unsuspected link between abnormal cAMP signaling and defective regulation of the inflammasome and suggest that caspase-1 and PGE2 inhibition may be therapeutic targets in bone lesions associated with defects of these two pathways.

INTRODUCTION

In humans and mouse models, inappropriate activation of the cyclic (c) adenosine-monophosphate (cAMP) signaling pathway leads to the development of bone lesions that vary from fibrous dysplasia (FD) to osteochondromyxomas (OCM) and chondro- and osteo-sarcomas (C/OS) (1–5). We and others have demonstrated that these lesions are derived from early progenitors of the osteoblastic lineage, bone stromal (also known as 'stem') cells (BSCs) (4,5).

Recently, similar lesions were described in children with neonatal-onset multisystem inflammatory disease (NOMID) (6). NOMID is caused by an abnormally increased activation of the potent pro-inflammatory cytokine interleukin-1β (IL1B); most NOMID patients carry mutations in *NLRP3*, the gene encoding cryopyrin (7,8). The latter is an essential

*To whom correspondence should be addressed at: Section on Endocrinology and Genetics, Program on Developmental Endocrinology and Genetics (PDEGEN), *Eunice Kennedy Shriver* National Institute of Child Health and Human Development (NICHD), National Institutes of Health (NIH), 10 Center Drive, Building 10, NIH-Clinical Research Center, Room 1-3216, MSC1103, Bethesda, MD 20892, USA. Tel: +1 3014964686; Fax: +1 3014020574; Email: stratakc@mail.nih.gov

component of the multimeric inflammasome complex that activates caspase-1, an enzyme that cleaves the inactive IL1B precursor (pro-IL1B) to its active form, IL1B (9). Caspase-1 plays a prominent role in inflammatory responses and the regulation of apoptosis of various tumor cells (10,11).

Approximately 60% of the NOMID patients have severe arthropathy that most commonly involves the knees (7). These patients occasionally develop bulky masses usually in the physis of the distal femur and the proximal tibia (6). These are typically the skeletal locations of lesions associated with abnormal cAMP signaling in both mice (1,5) and humans (2). The histology of NOMID bone lesions also shows similarities to FD and OCM: cartilage formation is disorganized at an area proximal to the growth plate; the nearby trabecular bone is undermineralized and appears to be less dense than normal, whereas proliferative fibrous tissue fills bone marrow space with several foci of irregular calcification (6). The molecular mechanisms underlying the development of bone lesions in NOMID patients are hitherto unknown.

Prompted by these histological similarities, we investigated the possibility that NOMID bone lesions could be associated with increased cAMP signaling. We also explored the hypothesis that inappropriate caspase-1 activation may be involved in the bone defects of patients with OCM and mice with extensive FD-like lesions and increased cAMP-dependent protein kinase [protein kinase A (PKA)] signaling, such as those that are haploinsufficient for the regulatory subunit type 1A of PKA (PRKAR1A) and the catalytic subunit α (PRKACA), the *Prkar1a*$^{+/-}$*Prkaca*$^{+/-}$ mice (5). Indeed, NOMID tumor cells showed high cAMP levels and increased PKA activity. Like in bone tumor cells from the *Prkar1a*$^{+/-}$ *Prkaca*$^{+/-}$ mice, NOMID tumor cells expressed human BSC markers and showed an enrichment of the *Wnt* signaling pathway in their gene signature. Our functional studies showed that PKA regulates caspase-1 expression through Ets-1. Both mouse and human bone tumor cells showed high prostaglandin E2 (PGE2) levels, a well-known stimulator of the cAMP/PKA pathway (12,13) and inhibitor of chondrocyte differentiation (14).

These data support the hypothesis that an increase in cAMP signaling through PKA leads to caspase-1 activation by Ets-1, at least in bone. This is the first time that cAMP and/or PKA is shown to have an effect on caspase-1, a finding that may have wider implications for the effects of cAMP on protein secretion that is regulated by caspase-1, as well as the potential regulation of the inflammasome by cAMP and/or PKA.

RESULTS

Ets-1 and caspase-1 are up-regulated in bone tumors due to PKA defects

The *Ets-1* gene, which plays an important role in cartilage and bone formation (15), was significantly over-expressed in *Prkar1a*$^{+/-}$ *Prkaca*$^{+/-}$ bone tumors when compared with bone from both single haploinsufficient animals (*Prkar1a*$^{+/-}$) and wild-type (WT) control littermate (Fig. 1A). Ets-1 was also highly expressed in *Prkar1a*$^{+/-}$ *Prkaca*$^{+/-}$ bone tumors at the protein level by western blot and immunohistochemistry (IHC) (Fig. 1B and C). The Ets-2 transcription factor, in contrast, was significantly less expressed in *Prkar1a*$^{+/-}$ *Prkaca*$^{+/-}$ bone tumors (Fig. 1B; Supplementary Material, Fig. S1).

Caspase-1 gene, which is known to be transcriptionally regulated by the Ets-1 proto-oncogene (10), was found to be over-expressed in *Prkar1a*$^{+/-}$ *Prkaca*$^{+/-}$ bone tumors both at the message and protein levels (Figs 1A and 2A and B). Cryopyrin, a protein highly expressed in polymorphonuclear cells and chondrocytes, forms a complex with pro-caspase-1 and the adaptor protein *pycard* (also known as ASC or apoptosis-associated speck-like protein containing a CARD domain) that leads to the activation of caspase-1. The inflammasome complex leads to the release of active caspase-1, which in turn activates IL1B through the cleavage of pro-IL1B (9,16). *Nlrp3* (the product of the cryopyrin gene) was over-expressed in *Prkar1a*$^{+/-}$ *Prkaca*$^{+/-}$ mice (Fig. 1A). IL1B expression was also significantly higher in *Prkar1a*$^{+/-}$*Prkaca*$^{+/-}$ mice at both the message (Fig. 1A) and protein levels (Fig. 2C).

We then studied human tumors (OCM) from patients with *PRKAR1A* defects. Unfortunately, the only material available was paraffin-embedded: ICH showed strong staining for ETS-1, IL1B and cryopyrin and less intense for caspase-1 (Supplementary Material, Fig. S2).

Characterization of NOMID non-lesional and tumor cells

Human bone cells were isolated by enzymatic digestion from a tumor-like bone lesion (NOMID tumor cells) and normal cartilage shavings (NOMID non-lesional cells) from the same patient with NOMID arthropathy (Fig. 3A). Two non-pathogenic variants (A242A, rs3806268 and S434S, rs34298354) in the *NLRP3* were found in leukocyte DNA from this patient. The BSC marker CD146 was increased in NOMID tumor cells compared with non-lesional cells (56.8 versus 40%; median fluorescent intensity, 976 versus 631; $\chi^2 = 19$, $P < 0.001$) (Fig. 3B).

Microarray analysis was performed in NOMID non-lesional and tumor cells using the *Illumina Beadarrays*® system. All genes were displayed in the heat maps constructed by processing the data using unsupervised hierarchical clustering (Fig. 3C), as described previously (17). The functional analysis of the whole-genome transcriptome profiling was performed using the DAVID Bioinformatic Resources 2008 (NIAID, NIH) (18) (Fig. 3D and Supplementary Material, Table S1). Gene set enrichment analysis was used to identify pathways associated with the NOMID-tumor signature; this revealed high statistical association with *Wnt* signaling in tumor cells compared with non-lesional cells isolated from the same patient ($P = 0.002$). In addition, apoptosis and glutamate metabolism pathways were over-expressed in NOMID tumor cells ($P = 0.003$ and $P = 0.004$, respectively).

PKA activity, cAMP levels and PKA subunit expression in NOMID cells

An increase in cAMP-stimulated kinase activity was detected in NOMID tumor cells when compared with NOMID non-lesional cells (163 991 $\pm$ 6222 versus 122 307 $\pm$ 2114; $P =$ 0.02). The former also had high cAMP levels (2.5 $\pm$ 0.2

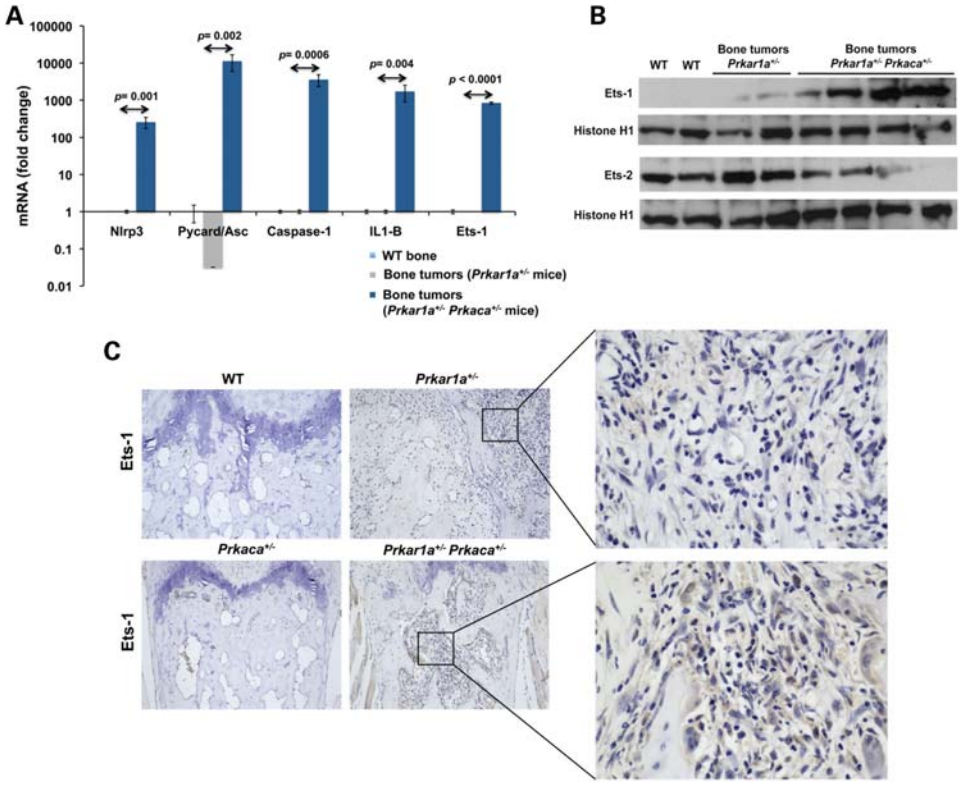

Figure 1. Ets-1 and caspase-1 inflammasome up-regulation in bone tumors from *Prkar1a*$^{+/-}$ *Prkaca*$^{+/-}$ mice. (**A**) Quantitative RT–PCR analysis showing *Nlrp3*, *ASC*, *Casp1*, *IL1b* and *Ets-1* over-expression in *Prkar1a*$^{+/-}$ *Prkaca*$^{+/-}$ bone tumors ($n = 3$) compared with *Prkar1a*$^{+/-}$ bone tumors ($n = 3$) and WT bone ($n = 3$). (**B**) Western blot analysis showing high Ets-1 protein levels and Ets-2 down-regulation in *Prkar1a*$^{+/-}$ *Prkaca*$^{+/-}$ bone tumors. Western blot analysis was performed in triplicate. (**C**) Strong positive staining for Ets-1 in bone tumor from *Prkar1a*$^{+/-}$ *Prkaca*$^{+/-}$ mice. *Prkar1a*$^{+/-}$ bone tumor and bone tissue from *Prkaca*$^{+/-}$ and WT mice displayed a negative staining (magnification, $\times 10$ and $\times 40$). Gene expression analysis is presented as mean $\pm$ SD.

versus 0.14 ± 0.05; $P < 0.001$) (Fig. 4A). To determine which type of PKA accounted for the higher PKA activity in NOMID tumor cells, we performed diethylaminoethyl (DEAE) cellulose ion-exchange column chromatography followed by elution with a linear sodium chloride gradient on total proteins extracted from NOMID non-lesional and bone tumor cells. The fractions were then measured for PKA type I (PKA-I) versus type II (PKA-II) activity: PKA-I complex was eluted between 40 and 80 mM of NaCl, whereas PKA-II complex was eluted between 180 and 270 mM of NaCl under these conditions. There were no free forms of regulatory or catalytic subunits under these ranges of NaCl concentration. Only PKA-I activity, and not PKA-II, was significantly higher in NOMID tumor cells ($P = 0.01$) (Fig. 4B).

We then assessed PKA regulatory and catalytic subunit expression. The regulatory subunits RIα and RIIα had similar protein levels in NOMID non-lesional and tumor cells, whereas RIIβ was undetectable (Fig. 4C). NOMID tumor cells showed expression of all PKA catalytic subunits (Cα, Cβ, Cγ and Prkx), with a relative increase in the Cβ subunit (Fig. 4D). In addition, NOMID tumor cells showed higher expression levels for both Ets-1 and, as expected, caspase-1 (Fig. 4E).

In summary, the higher PKA-I activity in NOMID tumor cells may be primarily explained by an increase in Cβ expression, the catalytic subunit that is primarily responsible for FD-like lesions and associated tumors in mice with PKA defects (5).

PKA regulates caspase-1 via Ets-1 proto-oncogene activation

To examine the role of PKA in the regulation of Ets-1 transcription factor, we analyzed the effects of specific siRNAs against the PKA regulatory and catalytic subunits in transiently transfected MC3T3 cells. MC3T3 cells are mouse preosteoblasts that express genes encoding BSC and other osteoblast markers (19,20). The down-regulation of the target genes by siRNAs was confirmed by western blot analysis.

Down-regulation of PKA regulatory subunits (RIα, RIIα and RIIβ) did not modify Ets-1 and caspase-1 expression (Supplementary Material, Fig. S3). The main PKA-I catalytic subunit is Cα coded by the *PRKACA* gene. We observed a dramatic reduction in Ets-1 and caspase-1 expression after transient transfection of the MC3T3 cells with catalytic subunit Cα siRNA (Fig. 5A). Cells transfected with Ets-1 siRNA also showed a reduction in caspase-1 expression, whereas Ets-2 down-regulation had no effect on caspase-1 protein levels (Fig. 5B). When cells were transfected with the *PRKACA*

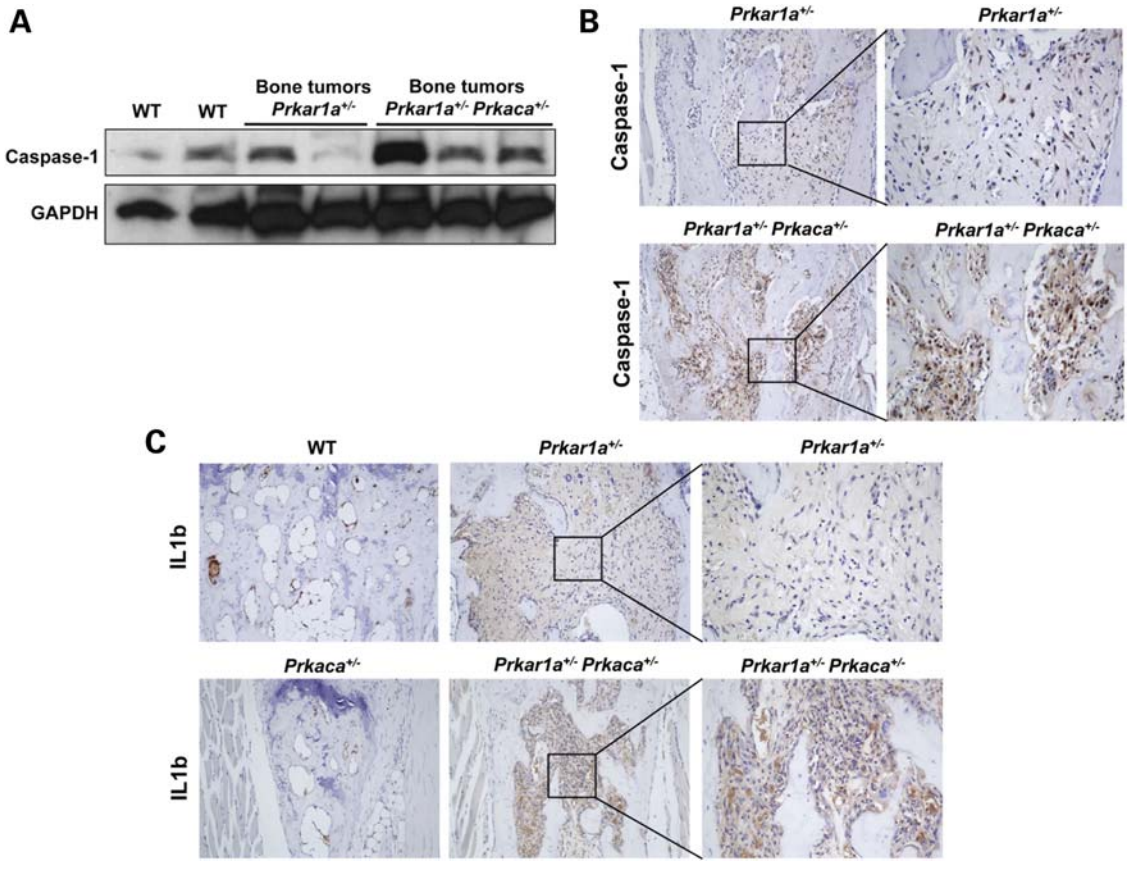

Figure 2. Caspase-1 and IL1B over-expression at the protein level in *Prkar1a*$^{+/-}$ *Prkaca*$^{+/-}$ bone tumors. (**A**) Caspase-1 protein levels were higher in bone tumors from *Prkar1a*$^{+/-}$ *Prkaca*$^{+/-}$ mice than from *Prkar1a*$^{+/-}$ and WT mice (western blot analysis was performed in triplicate). (**B**) Stronger caspase-1 immunoreactivity in *Prkar1a*$^{+/-}$ *Prkaca*$^{+/-}$ bone tumor when compared with *Prkar1a*$^{+/-}$ bone lesion (magnification, ×10 and ×20). (**C**) *Prkar1a*$^{+/-}$ *Prkaca*$^{+/-}$ bone tumor cells inside the bone marrow cavity displayed a high staining for IL1B (magnification, ×10 and ×40).

expressing vector, a significant increase in the Ets-1 and caspase-1 protein expression was seen (Fig. 5C).

To investigate whether the Cα subunit increased Ets-1 and caspase-1 expression by inhibition of proteosome degradation, Cα siRNA-transfected cells were treated with clasto-lactacystin β-lactone, a proteosome proteolytic activity inhibitor (21). Clasto-lactacystin β-lactone treatment did not rescue Ets-1 and caspase-1 down-regulation after Cα siRNA transfection (Fig. 5A).

Given the fact that ETS-1 trans-activation is mediated by cAMP-responsive element-binding (CREB) protein (22), we hypothesized that caspase-1 activation by PKA is regulated through Ets-1. To address this question, we performed simultaneous transfections with the *PRKACA*-expressing vector and Ets-1 siRNA (Fig. 5C). Ets-1 down-regulation in cells transfected with the *PRKACA* vector blocked significantly the increase in caspase-1 expression that was induced by PRKACA alone.

Ets-1 and caspase-1 expression are regulated by cAMP via PKA

Next, we investigated the effect of cAMP levels on the expression of Ets-1 and inflammasome molecular partners in MC3T3 cells. A significant increase in *Nlrp3*, *Caspase-1* and *Ets-1* expression was observed after treatment with forskolin 10 μM (Supplementary Material, Fig. S4A). To evaluate whether cAMP effects on *Nlrp3*, *Caspase-1* and *Ets-1* expression were mediated primarily by PKA, cells were treated with low concentrations of the PKA inhibitor H89. The inhibition of PKA activity blocked the increase in the *Nlrp3*, *Caspase-1* and *Ets-1* expression stimulated by cAMP (Supplementary Material, Fig. S4A). After 6 h of *forskolin* treatment, an increase in Ets-1 and caspase-1 expression was demonstrated by western blot (Supplementary Material, Fig. S4B). Similarly, the PKA inhibitor H89 also blunted the cAMP effects on Ets-1 and caspase-1 expression at protein levels.

High PGE2 levels in mouse and NOMID tumor cells

We have recently shown that cAMP levels are increased in the *Prkar1a*$^{+/-}$ and *Prkar1a*$^{+/-}$*Prkaca*$^{+/-}$ mouse bone tumor cells (5), and here (see above) we also showed that NOMID tumor cells have high cAMP levels. PGE2 is a well-known activator of cAMP/PKA signaling (12,13) and a relevant inhibitor of chondrocyte differentiation (14). In addition, the main enzymes leading to PGE2 elevation, cyclooxygenase-2 (COX-2) and microsomal prostaglandin E synthase-1 (mPGES-1) are induced by IL1B (23). As caspase-1 is a key

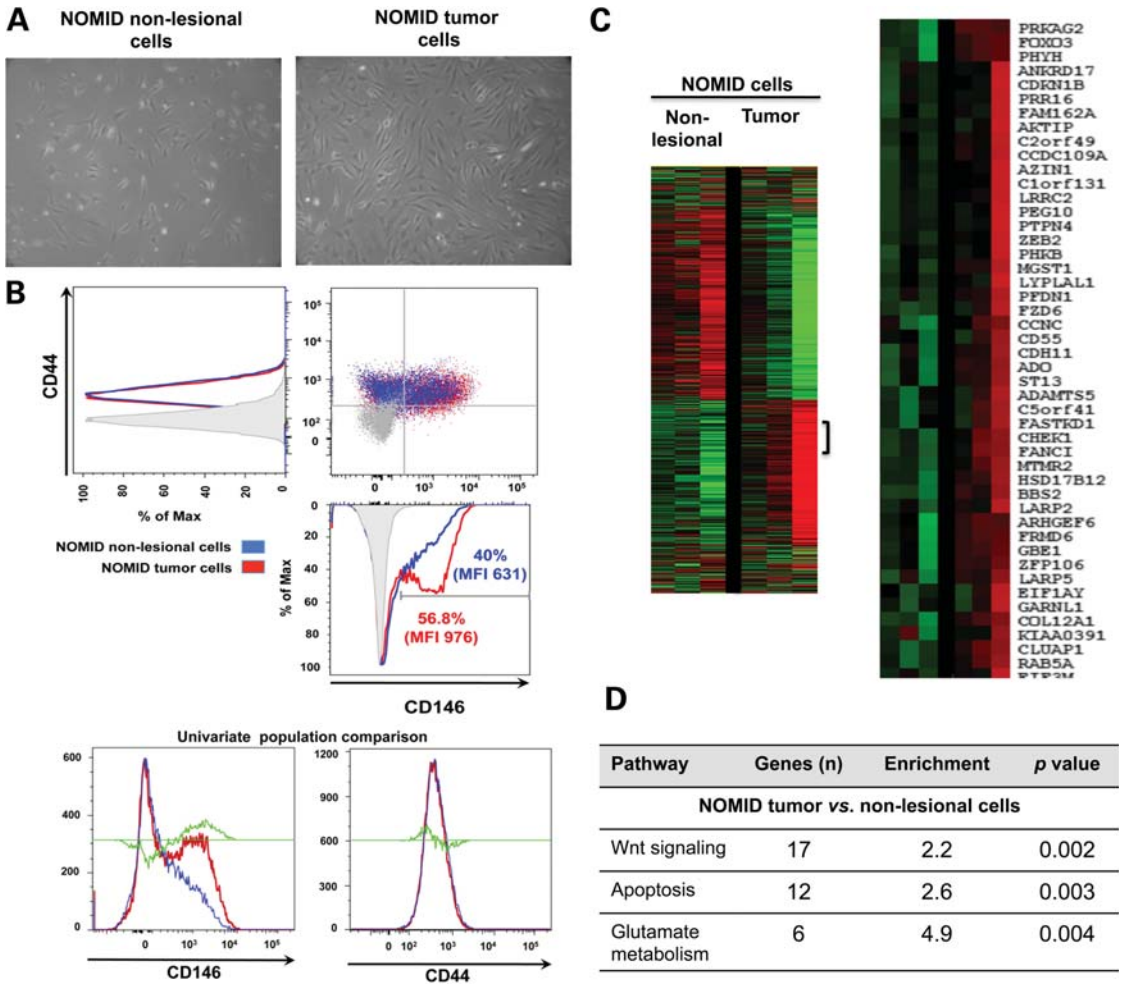

Pathway	Genes (n)	Enrichment	*p* value
NOMID tumor *vs.* non-lesional cells			
Wnt signaling	17	2.2	0.002
Apoptosis	12	2.6	0.003
Glutamate metabolism	6	4.9	0.004

Figure 3. Molecular characterization of NOMID cells . (**A**) NOMID cells have a fibroblastoid and spindle-shaped appearance at phase contrast microscopy (magnification, ×10). (**B**) The BSC marker CD146 was increased in NOMID tumor cells compared with NOMID non-lesional cells. (**C**) Heatmap visualization of gene expression data from NOMID non-lesional and tumor cells. (**D**) Functional analysis of whole-genome transcriptome profiling showing up-regulation of Wnt signaling and apoptosis pathways in NOMID tumor cells. BSC, bone stem cell; MFI, median fluorescent intensity.

regulator of IL1B synthesis, and in this study both NOMID and cells from mice with PKA defects showed activated caspase-1, we measured PGE2 levels in cell culture medium from human NOMID and mouse *Prkar1a*$^{+/-}$ and *Prkar1a*$^{+/-}$ *Prkaca*$^{+/-}$ bone tumor cells. Indeed, PGE2 levels were significantly higher in *Prkar1a*$^{+/-}$ and *Prkar1a*$^{+/-}$ *Prkaca*$^{+/-}$ bone tumor cells (691.5 ± 130 and 698.7 ± 23 pg/ml, respectively) when compared with MC3T3 cells (46.3 ± 2.3 pg/ml; $P < 0.05$) (Fig. 6A). NOMID tumor cells also showed higher PGE2 levels than NOMID non-lesional cells (337.6 ± 13.7 versus 32.3 ± 1.8 pg/ml, respectively; $P < 0.05$) (Fig. 6B).

Caspase-1 and PGE2 inhibition decrease proliferation of cells with PKA and NOMID defects

We then investigated the role of caspase-1 activation in the proliferation of bone tumor cells *in vitro*. We used Ac-YVAD-CMK, a selective and irreversible caspase-1 inhibitor (24). Caspase-1 inhibition significantly reduced proliferation at 43 ± 6.8% of *Prkar1a*$^{+/-}$ *Prkaca*$^{+/-}$ bone tumor cells at 48 h of treatment (Fig. 6C). The caspase inhibitor had no significant effect on MC3T3 and *Prkar1a*$^{+/-}$ cells. NOMID non-lesional and tumor cells also showed a dramatic reduction in proliferation at 60 ± 6.1 and 83 ± 2.7%, respectively, after 48 h of treatment with the caspase-1 inhibitor (Fig. 6D). In addition, the inhibition of PGE2 production through the selective modulation of mPGES-1 expression significantly reduced the viability of *Prkar1a*$^{+/-}$ and *Prkar1a*$^{+/-}$*Prkaca*$^{+/-}$ bone tumor cells after 48 h of treatment (92 ± 1.6 and 93 ± 1.4%, respectively) (Fig. 6E). Finally, the blockage of PGE2 synthesis led to a progressive reduction on proliferation of NOMID non-lesional and tumor cells (Fig. 6F).

DISCUSSION

Our recent studies showed that *Prkar1a*$^{+/-}$*Prkaca*$^{+/-}$ mice developed bone tumors that bore histological resemblance to those that develop in humans with NOMID (5). *Prkar1a*$^{+/-}$

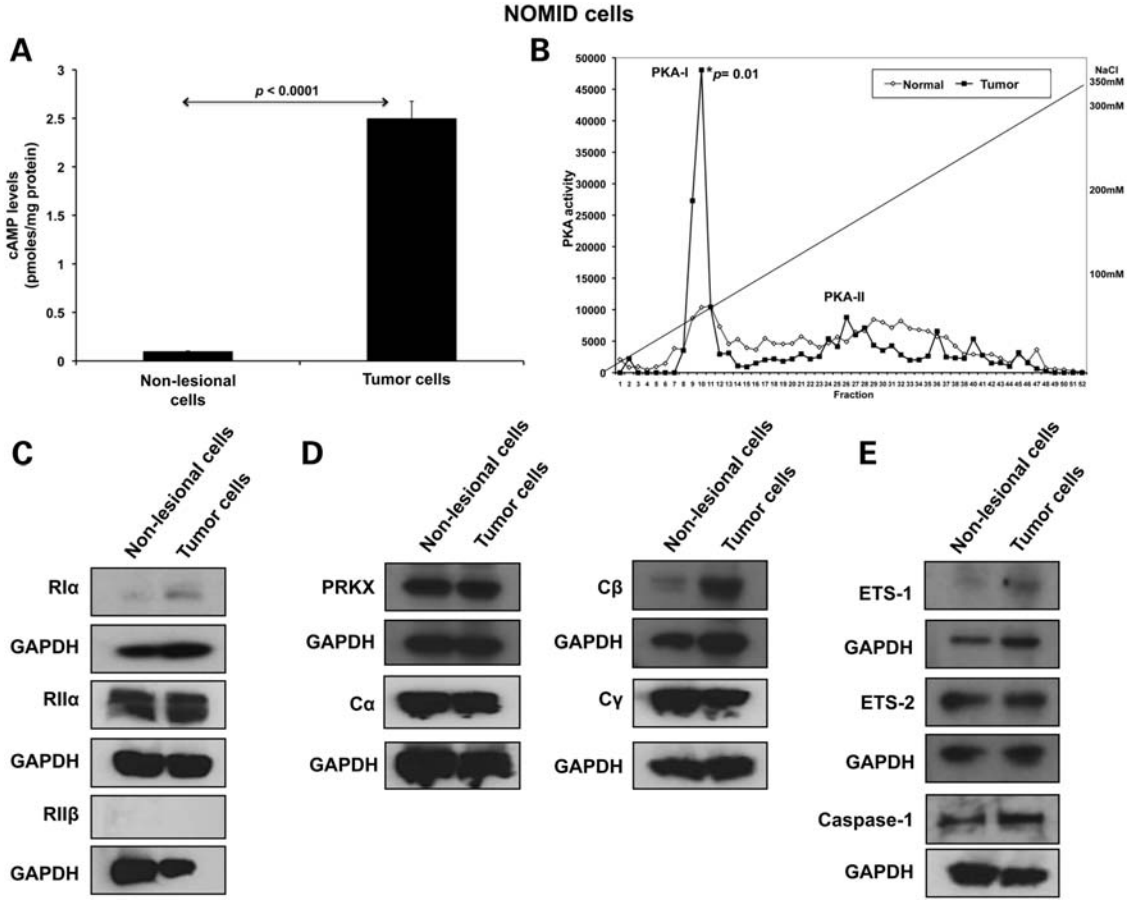

Figure 4. High PKA activity, cAMP levels and β catalytic subunit (Cβ) expression in NOMID tumor cells. (**A**) NOMID tumor cells presented high cAMP levels when compared with NOMID non-lesional cells. (**B**) PKA-I activity after cAMP stimulus was significantly higher in NOMID tumor cells than in non-lesional cells ($P = 0.01$). (**C**) RIα and RIIα protein levels were similar in NOMID non-lesional and tumor cells. (**D**) NOMID tumor cells showed a remarkable induction in the expression of Cβ subunit. Expression levels of the other catalytic subunits (Cα, Cγ and Prkx) were similar in NOMID non-lesional and tumor cells. (**E**) NOMID tumor cells presented higher expression levels of Ets-1 and caspase-1. All the experiments (cAMP and PKA assays and western blot analysis) were performed in triplicate. cAMP levels are presented as mean ± SD.

Prkaca$^{+/-}$ mouse lesions involved a particular subpopulation of cells that could be identified as belonging to the osteoblastic lineage, derived from stromal cells (BSCs), and were localized in specific locations of the skeleton always proximal to the growth plate (5). The present study suggests that NOMID bone tumors are also derived from the homologous, if not identical, cells that are cAMP/PKA-sensitive and proliferate in the same skeletal areas that are affected in humans and mice with PKA defects.

The molecular mechanism shared by the two very distinct disorders was elucidated in this report and was hitherto unsuspected: cAMP/PKA activates caspase-1 via the transcription factor Ets-1; this leads to increased IL1B and consequently PGE2, which in turn increases cAMP levels further, feeding into a vicious cycle of PKA and caspase-1 activation within the affected bone tissues. This could explain the histological features of a PKA defect-like condition in NOMID; it also led to the identification of PGE2 as the main culprit behind the increased cAMP levels in human and mouse bone lesions with PKA defects.

What is remarkable in the identified cross-talk between the two pathways is that each can activate the other outside of their usual context: caspase-1 activation in cells with PKA defects was associated with an increase in cAMP levels and further activation of the PKA pathway (employing PGE2), without the involvement of any other exogenous signals. Vice versa, PKA activation of caspase-1 in NOMID cells led to IL1B and PGE2 increases without any need for activation of pro-inflammatory markers. It should be noted that in both human (2,6) and mouse (1,5) bone tumors caused by NOMID or PKA defects, there was never any histological or other evidence of inflammation. Arthropathy in NOMID is not caused by synovitis or joint effusion, but by abnormal endochondral bone formation and defective chondrocyte apoptosis (25,26). Lack of inflammation in NOMID bone tumors was somewhat of a puzzle in this pro-inflammatory condition, but it can now easily be explained by the findings of this study.

Another novel finding of this investigation is the regulation of Ets-1 by PKA. The Ets family of proteins consists of a large number of evolutionarily conserved transcription factors, and inappropriate expression of ETS-1 has been linked to a variety of human cancers (27). ETS-1 is known to transform cell lines, promote autonomous growth in culture and lead to tumor formation *in vivo* (28–30). Ets-1 mRNA is first detected

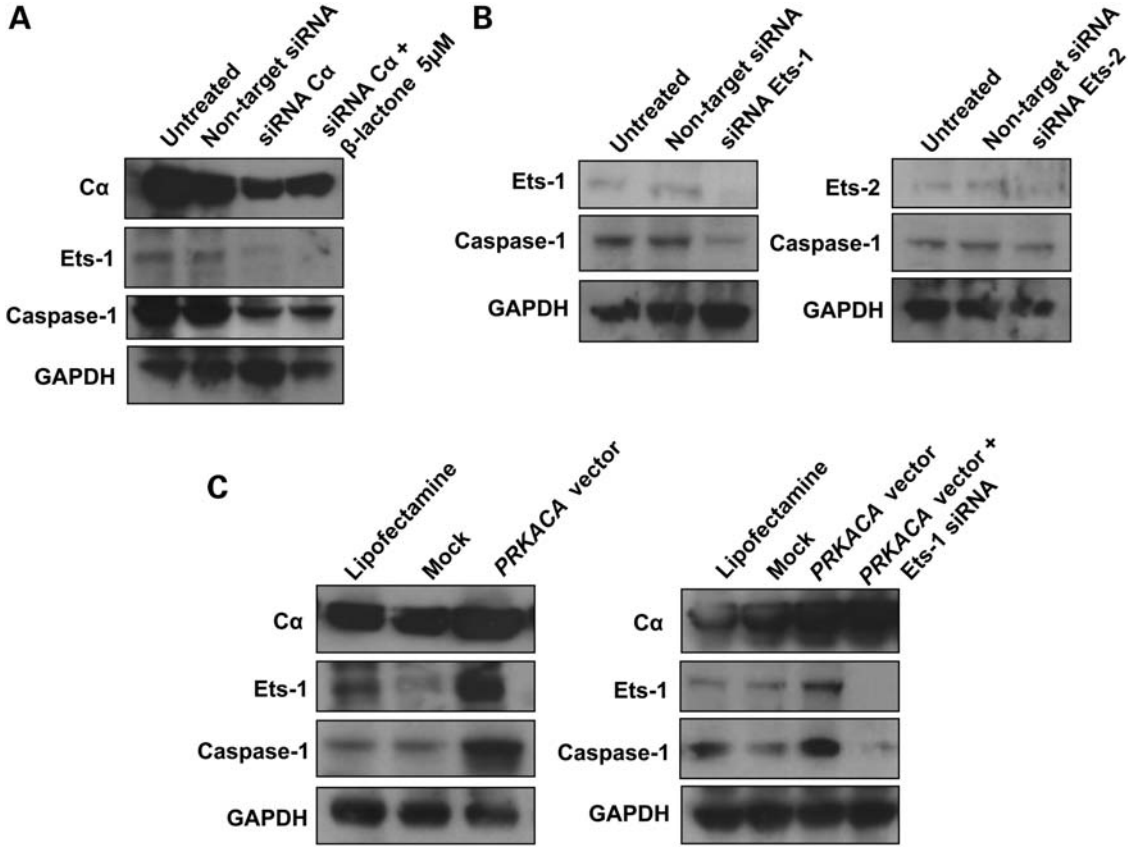

Figure 5. Protein kinase A regulates caspase-1 via Ets-1 proto-oncogene activation . (**A**) Ets-1 and caspase-1 expression had a significant down-regulation after transient transfection with Cα siRNA. (**B**) Western blot analysis showed a reduction in caspase-1 expression in MC3T3 cells transfected with Ets-1 siRNA. Ets-2 down-regulation had no effect on caspase-1 protein expression. (**C**) PRKACA-expressing vector promoted a significant increase in the Ets-1 and caspase-1 protein expression. Simultaneous transfection with Ets-1 siRNA and *PRKACA*-expressing vector blocked caspase-1 up-regulation induced by Cα subunit. Western blot analysis was confirmed in three independent experiments.

at day 14 of mouse development in mesenchymal cells in the developing limbs, tail, vertebrate and other sites (31), where bone development occurs and where tumors in NOMID and PKA defects occur. During bone formation, Ets-1 and Ets-2 peak at different stages: Ets-1 is expressed in mesenchymal cells (31) regulating genes that are involved in proliferation, whereas Ets-2 expression peaks during osteoblast differentiation and matrix maturation (32). The signal transduction pathways that regulate ETS-1 expression in bone were unknown. In this study, we showed that PKA regulates caspase-1 expression through Ets-1 activation. Caspase-1 up-regulation induced by PKA was blocked by Ets-1 down-regulation, suggesting a direct effect of PKA on Ets-1 transcription. Ets-1 transactivation requires the recruitment of p300 and CREB protein (22,33). It was known that Ets-1 activates the transcription of caspase-1 by direct binding to a functional activation site in the caspase-1 promoter (10).

The findings of this study have important implications for therapeutics, since the two pathways can now be targeted interchangeably (or, maybe, simultaneously) in bone lesions associated with either PKA defects or NOMID. Almost all NOMID manifestations (fever, urticarial rash, aseptic meningitis and arthropathy) are driven by increased IL1B and respond to the systemic administration of *anakinra*, an IL-1 antagonist (34). In this study, we showed that inhibition of caspase-1, the enzyme that cleaves pro-IL1B to its active form IL1B, significantly decreased proliferation of both NOMID cells and *Prkar1a*$^{+/-}$*Prkaca*$^{+/-}$ bone tumor cells, suggesting that this drug may be helpful in controlling manifestations of patients with PKA defects as well.

Increased IL1B expression in both NOMID and *Prkar1a*$^{+/-}$ *Prkaca*$^{+/-}$ bone tumor cells was also associated with increased PGE_2 through induction of COX-2 and mPGES-1 protein expression. Dysregulation of the COX-2/PGE_2 pathway plays a key role in the development of many tumors (35), and it has been demonstrated that human mesenchymal stem cell proliferation is regulated by PGE_2 through activation of cAMP-dependent PKA-I (12), consistent with the findings in this study. PGE_2 suppresses the maturation of growth plate chondrocytes and inhibits the expression of *colX*, *VEGF*, *MMP-13* and *alkaline phosphatase* in a dose-dependent manner (14). PGE_2 rapidly activates CREB through PKA signaling and results in the subsequent transcriptional activation of PKA/CREB-dependent genes (14). Interactions between PGE_2 and Wnt signaling pathway regulate proliferation and regeneration of stem cells. PGE_2 modifies the Wnt signaling cascade at the level of β-catenin degradation through cAMP/PKA (13). Indeed, the gene signature

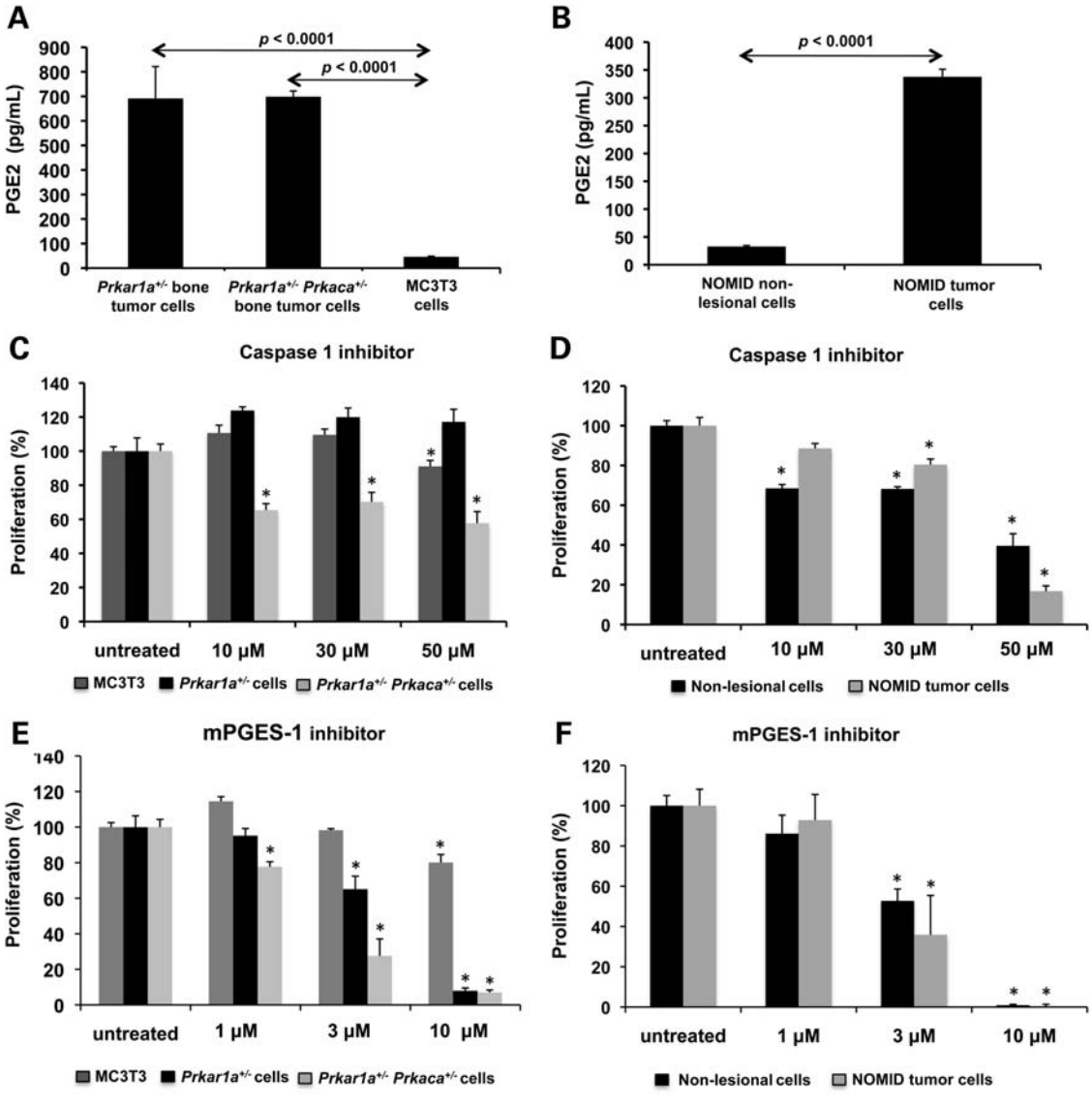

Figure 6. Mouse and NOMID tumor cells secret PGE2 and show high sensibility to caspase-1 and mPGES-1 inhibition. (**A**) PGE2 levels were significantly higher in *Prkar1a*$^{+/-}$ and *Prkar1a*$^{+/-}$ *Prkaca*$^{+/-}$ bone tumor cells when compared with MC3T3 cells. (**B**) NOMID tumor cells also showed higher PGE_2 levels than NOMID non-lesional cells. (**C**) Caspase-1 inhibition significantly reduced proliferation of *Prkar1a*$^{+/-}$ *Prkaca*$^{+/-}$ bone tumor cells. The caspase inhibitor had no effect on MC3T3 cells and *Prkar1a*$^{+/-}$ bone tumor cells. (**D**) NOMID cells showed a significant decrease in proliferation after caspase-1 inhibition. (**E**) The inhibition of PGE2 production by a selective inhibitor of mPGES-1 significantly reduced viability of *Prkar1a*$^{+/-}$ and *Prkar1a*$^{+/-}$ *Prkaca*$^{+/-}$ bone tumor cells. (**F**) NOMID non-lesional and tumor cells also had a progressive reduction on proliferation after mPGES-1 blockage. PGE2 levels and cell proliferation are shown as mean ± SD. All the experiments were performed in triplicate. PGE2, prostaglandin E2; mPGES1, microsomal prostaglandin E synthase-1.

of NOMID tumor-like bone lesion cells showed a significant enrichment with expression of genes of the Wnt signaling pathway, similar to what we have shown elsewhere for PKA subunit defects (36–38). Interestingly, Wnt signaling activation is shared by all human lesions and mouse tissues affected by increased cAMP signaling that we have studied so far (37,39–41). Thus, COX2-, PGE2- and/or Wnt inhibitors can potentially be useful in the treatment of patients with the NOMID arthropathy.

In conclusion, we identified a key link between cAMP signaling and the inflammasome in bone cells (Fig. 7). This finding has potentially more general implications, such as, for example, on the possible effect of cAMP on caspase-1-mediated regulation of protein secretion. It may also lead to new therapies in patients with NOMID or those with PKA defects.

MATERIALS AND METHODS

Animal studies

Prkar1a heterozygous mice (*Prkar1a*$^{+/-}$), which contain one null allele of *Prkar1a*$^{\Delta 2}$, were generated previously in our laboratory (1). *Prkaca* heterozygous mice (*Prkaca*$^{+/-}$), which have a neomycin resistance cassette to replace exons 6–8 of the *Prkaca* gene (42), were purchased from Mutant Mouse

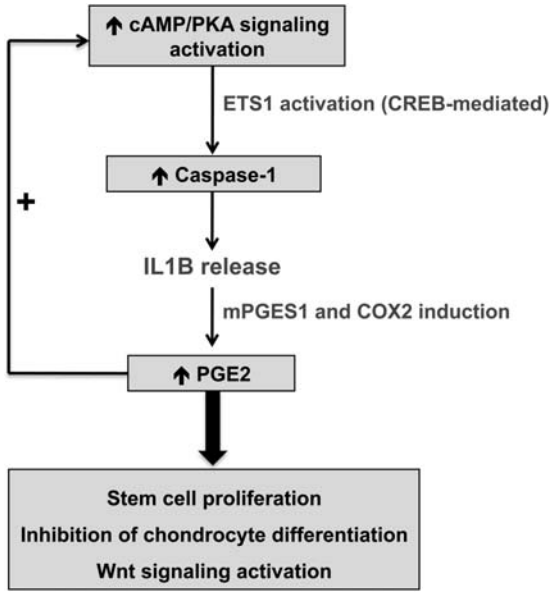

Figure 7. Schematic representation of pro-inflammatory pathway induction by cAMP/PKA signaling in BSC-derived lesions. PGE2, prostaglandin E2; mPGES1, microsomal prostaglandin E synthase-1; COX2, cyclooxygenase-2; CREB, cAMP-responsive element-binding protein.

Regional Resource Centers (strain name: B6; 129X1-Prkacatm1Gsm/Mmnc). *Prkar1a*$^{+/-}$ and *Prkaca*$^{+/-}$ mice were crossed to generate *Prkar1a*$^{+/-}$*Prkaca*$^{+/-}$ mice on a mixed C57BL/6 129Sv/B6 hybrid background (5). All animals were genotyped as described previously. Animal work in this study was carried out in accordance with Institutional Laboratory Animal Care and Use Committee guidelines under animal protocol 06-033 (at the NIH, Bethesda, MD, USA).

Primary cell cultures

Primary culture of *Prkar1a*$^{+/-}$ and *Prkar1a*$^{+/-}$ *Prkaca*$^{+/-}$ bone tumors was established as described previously (5). Tissues from the bone lesion and non-affected cartilage of a same patient with NOMID were isolated from cartilage shavings by enzymatic digestion (43).

Microarray analysis

Total RNA was extracted from NOMID non-lesional and tumor cells using the *TRIZOL* reagent method. Three biological replicates for each of the two cell lines were used for microarray analysis. Preparation of cRNA from total RNA, hybridization in Expression BeadChips, scanning and image analysis were done as described previously (44). Normalization and analysis of microarray data were performed as described previously (37). The raw and normalized microarray data reported in this paper have been deposited in the Gene Expression Omnibus database (accession no. GSE21835).

Real-time quantitative RT–PCR

Quantitative real-time PCR was performed in the ABI Prism 7700 Sequence Detector using TaqMan Gene Expression Assays according to the manufacturer's instructions (Applied Biosystems, Foster City, CA, USA). The assay IDs were Nlrp3, Mm00840904_m_1; ASC, Mm00445747_g_1; Casp1 Mm00438023_m_1; Il1b Mm00434228_m_1 and Ets-1 Mm00468970_m_1, GAPDH 4308313. The relative quantification was performed using the $2^{-\Delta\Delta CT}$ method (45).

siRNA and construct transfections

MC3T3 cells were transfected with 100 nM MISSION® siRNA (Sigma-Aldrich, St Louis, MO, USA) specific to mouse RIα (SASI_Mm01_00116787), RIIα (SASI_Mm01_00122100), RIIβ (SASI_Mm01_00163961), Cα (SASI_Mm01_00217223), Ets-1 (SASI_Mm01_00173246), Ets-2 (SASI_Mm01_00130872) or non-targeting pool siRNA using N-TER peptide transfection reagent (Sigma-Aldrich), as per manufacturer's instruction. Cα siRNA-transfected cells were treated with clasto-lactacystin β-lactone (5 μM), a proteosome proteolytic activity inhibitor (21).

MC3T3 cells were also transfected with the retroviral vectors OT1521 (mock) or OT1529 (*PRKACA*-expressing vector) containing the internal inducible mouse metallothionine-1 promoter driving the expression of construct for PKA subunits Cα, as described previously (46). All experiments were performed in triplicate.

Western blot analysis

Western blot analysis was performed following standard procedures (5,47). The following primary antibodies were used: RIα (610610, BD transduction), RIIα (C-20, Santa Cruz Biotechnology, Santa Cruz, CA, USA), RIIβ (H-90, Santa Cruz Biotechnology), Cα (C-20, Santa Cruz Biotechnology), Cβ (C-20), PRKX (a gift from Dr Robert M. Kotin, NHLBI, NIH, Bethesda, MD, USA), caspase-1 (M-20, Santa Cruz Biotechnology), Ets-1 (ab26096, Abcam, Cambridge, MA, USA), Ets-2 (C-20, Santa Cruz Biotechnology), GAPDH (ab9485, Abcam) and histone H1 (FL-219, Santa Cruz Biotechnology).

Immunohistochemistry

All IHC was performed in collaboration with Histoserv, Inc. (Germantown, MD, USA). The following primary antibodies were used: Ets-1 (ab26096, Abcam), Ets-2 (C-20, Santa Cruz Biotechnology), caspase-1 (M-20, Santa Cruz Biotechnology) and IL1B (H-153, Santa Cruz Biotechnology).

Flow cytometry

NOMID normal and tumor cells (1×10^5) were collected from cultures and fixed using BD Cytofix/Cytoperm™ Fixation/Permeabilization Solution Kit (BD Biosciences, San Jose, CA, USA). Subsequently, NOMID cells were stained with PE or fluorescein isothiocyanate (FITC)-tagged primary antibodies (CD44-FITC and CD146-PE, BD Biosciences) at 4°C for 30 min.

PKA activity, cAMP assay and DEAE cellulose chromatography

PKA enzymatic activity was measured as described previously (48). cAMP levels were determined by ^{3}H Biotrak Assay System (Amersham Biosciences, Piscataway, NJ, USA). DEAE cellulose chromatography was performed as described in Cheadle *et al*. (44).

Cell treatment, proliferation assay and PGE2 levels

MC3T3 cells were stimulated by forskolin (10 μM) associated or not with the PKA activity inhibitor H89 (50 nM). MC3T3, mouse (*Prkar1a*$^{+/-}$ and *Prkar1a*$^{+/-}$ *Prkaca*$^{+/-}$) bone tumor cells and NOMID cells were treated with Ac-YVAD-CMK (10, 30 and 50 μM; Cayman Chemical, Ann Arbor, MI, USA), a selective and irreversible caspase-1 inhibitor (24), or with CAY1052 (1,3 and 10 μM; Cayman Chemical), a selective mPGES-1 inhibitor (49). After 48 h of treatment, cell proliferation was evaluated using the CellTiter 96® AQueous One Solution Cell Proliferation Assay (Promega, Madison, WI, USA). PGE_2 concentration was measured in the cell culture medium using the Prostaglandin E2 ELISA Kit-Monoclonal (Cayman Chemical).

Statistical analysis

All statistical analyses were performed with SPSS 16.0 (SPSS Inc., Chicago, IL, USA). Continuous data are expressed as mean ± SD. All experiments were performed in triplicate. A two-sample *t*-test was used for paired samples. The Kolmogorov–Smirnov (K–S) test was employed to analyze the differences between NOMID tumor and normal cells at the flow cytometry. A *P*-value less than 0.05 was considered significant.

SUPPLEMENTARY MATERIAL

Supplementary Material is available at *HMG* online.

ACKNOWLEDGEMENTS

We would like to thank Dr Xibin Wang and Dr Hang Pham for their help with the NOMID cell line experiments. We also thank Dr J. Aidan Carney (Mayo Clinic, Rochester, MN, USA) for providing samples of human tumors associated with CNC.

Conflict of Interest statement. The authors have nothing to disclose.

FUNDING

This work was supported by US National Institutes of Health, Eunice Kennedy Shriver National Institute of Child Health and Human Development intramural project Z01-HD-000642-04 (to C.A.S.) and the NIAMS Intramural Research. Recent data (50) add support to PKA and/or involvement of *Prkar1a* in early osteoblast proliferation, and this pathway's significant involvement in human osteosarcoma. It would be interesting to study caspase-1 and/or the inflammasome in this human tumor.

REFERENCES

1. Kirschner, L.S., Kusewitt, D.F., Matyakhina, L., Towns, W.H. II, Carney, J.A., Westphal, H. and Stratakis, C.A. (2005) A mouse model for the Carney complex tumor syndrome develops neoplasia in cyclic AMP-responsive tissues. *Cancer Res.*, **65**, 4506–4514.
2. Carney, J.A., Boccon-Gibod, L., Jarka, D.E., Tanaka, Y., Swee, R.G., Unni, K.K. and Stratakis, C.A. (2001) Osteochondromyxoma of bone: a congenital tumor associated with lentigines and other unusual disorders. *Am. J. Surg. Pathol.*, **25**, 164–176.
3. Stratakis, C.A., Kirschner, L.S. and Carney, J.A. (2001) Clinical and molecular features of the Carney complex: diagnostic criteria and recommendations for patient evaluation. *J. Clin. Endocrinol. Metab.*, **86**, 4041–4046.
4. Pavel, E., Nadella, K., Towns, W.H. II and Kirschner, L.S. (2008) Mutation of Prkar1a causes osteoblast neoplasia driven by dysregulation of protein kinase A. *Mol. Endocrinol.*, **22**, 430–440.
5. Tsang, K.M., Starost, M.F., Nesterova, M., Boikos, S.A., Watkins, T., Almeida, M.Q., Harran, M., Li, A., Collins, M.T., Cheadle, C. *et al.* (2010) Alternate protein kinase A activity identifies a unique population of stromal cells in adult bone. *Proc. Natl Acad. Sci. USA*, **107**, 8683–8688.
6. Hill, S.C., Namde, M., Dwyer, A., Poznanski, A., Canna, S. and Goldbach-Mansky, R. (2007) Arthropathy of neonatal onset multisystem inflammatory disease (NOMID/CINCA). *Pediatr. Radiol.*, **37**, 145–152.
7. Aksentijevich, I., Nowak, M., Mallah, M., Chae, J.J., Watford, W.T., Hofmann, S.R., Stein, L., Russo, R., Goldsmith, D., Dent, P. *et al.* (2002) *De novo* CIAS1 mutations, cytokine activation, and evidence for genetic heterogeneity in patients with neonatal-onset multisystem inflammatory disease (NOMID): a new member of the expanding family of pyrin-associated autoinflammatory diseases. *Arthritis Rheum.*, **46**, 3340–3348.
8. Feldmann, J., Prieur, A.M., Quartier, P., Berquin, P., Certain, S., Cortis, E., Teillac-Hamel, D., Fischer, A. and de Saint Basile, G. (2002) Chronic infantile neurological cutaneous and articular syndrome is caused by mutations in CIAS1, a gene highly expressed in polymorphonuclear cells and chondrocytes. *Am. J. Hum. Genet.*, **71**, 198–203.
9. Petrilli, V., Dostert, C., Muruve, D.A. and Tschopp, J. (2007) The inflammasome: a danger sensing complex triggering innate immunity. *Curr. Opin. Immunol.*, **19**, 615–622.
10. Pei, H., Li, C., Adereth, Y., Hsu, T., Watson, D.K. and Li, R. (2005) Caspase-1 is a direct target gene of ETS1 and plays a role in ETS1-induced apoptosis. *Cancer Res.*, **65**, 7205–7213.
11. Mouawad, R., Antoine, E.C., Gil-Delgado, M., Khayat, D. and Soubrane, C. (2002) Serum caspase-1 levels in metastatic melanoma patients: relationship with tumour burden and non-response to biochemotherapy. *Melanoma Res.*, **12**, 343–348.
12. Kleiveland, C.R., Kassem, M. and Lea, T. (2008) Human mesenchymal stem cell proliferation is regulated by PGE2 through differential activation of cAMP-dependent protein kinase isoforms. *Exp. Cell Res.*, **314**, 1831–1838.
13. Goessling, W., North, T.E., Loewer, S., Lord, A.M., Lee, S., Stoick-Cooper, C.L., Weidinger, G., Puder, M., Daley, G.Q., Moon, R.T. *et al.* (2009) Genetic interaction of PGE2 and Wnt signaling regulates developmental specification of stem cells and regeneration. *Cell*, **136**, 1136–1147.
14. Li, T.F., Zuscik, M.J., Ionescu, A.M., Zhang, X., Rosier, R.N., Schwarz, E.M., Drissi, H. and O'Keefe, R.J. (2004) PGE2 inhibits chondrocyte differentiation through PKA and PKC signaling. *Exp. Cell Res.*, **300**, 159–169.
15. Raouf, A. and Seth, A. (2000) Ets transcription factors and targets in osteogenesis. *Oncogene*, **19**, 6455–6463.
16. Ting, J.P., Willingham, S.B. and Bergstralh, D.T. (2008) NLRs at the intersection of cell death and immunity. *Nat. Rev. Immunol.*, **8**, 372–379.
17. Eisen, M.B., Spellman, P.T., Brown, P.O. and Botstein, D. (1998) Cluster analysis and display of genome-wide expression patterns. *Proc. Natl Acad. Sci. USA*, **95**, 14863–14868.

18. Huang da, W., Sherman, B.T. and Lempicki, R.A. (2009) Systematic and integrative analysis of large gene lists using DAVID bioinformatics resources. *Nat. Protoc.*, **4**, 44–57.
19. Quarles, L.D., Yohay, D.A., Lever, L.W., Caton, R. and Wenstrup, R.J. (1992) Distinct proliferative and differentiated stages of murine MC3T3-E1 cells in culture: an *in vitro* model of osteoblast development. *J. Bone Miner. Res.*, **7**, 683–692.
20. Sudo, H., Kodama, H.A., Amagai, Y., Yamamoto, S. and Kasai, S. (1983) *In vitro* differentiation and calcification in a new clonal osteogenic cell line derived from newborn mouse calvaria. *J. Cell Biol.*, **96**, 191–198.
21. Dick, L.R., Cruikshank, A.A., Destree, A.T., Grenier, L., McCormack, T.A., Melandri, F.D., Nunes, S.L., Palombella, V.J., Parent, L.A., Plamondon, L. *et al.* (1997) Mechanistic studies on the inactivation of the proteasome by lactacystin in cultured cells. *J. Biol. Chem.*, **272**, 182–188.
22. Yang, C., Shapiro, L.H., Rivera, M., Kumar, A. and Brindle, P.K. (1998) A role for CREB binding protein and p300 transcriptional coactivators in Ets-1 transactivation functions. *Mol. Cell Biol.*, **18**, 2218–2229.
23. Park, J.Y., Pillinger, M.H. and Abramson, S.B. (2006) Prostaglandin E2 synthesis and secretion: the role of PGE2 synthases. *Clin. Immunol.*, **119**, 229–240.
24. Rabuffetti, M., Sciorati, C., Tarozzo, G., Clementi, E., Manfredi, A.A. and Beltramo, M. (2000) Inhibition of caspase-1-like activity by Ac-Tyr-Val-Ala-Asp-chloromethyl ketone induces long-lasting neuroprotection in cerebral ischemia through apoptosis reduction and decrease of proinflammatory cytokines. *J. Neurosci.*, **20**, 4398–4404.
25. Masumoto, J., Dowds, T.A., Schaner, P., Chen, F.F., Ogura, Y., Li, M., Zhu, L., Katsuyama, T., Sagara, J., Taniguchi, S. *et al.* (2003) ASC is an activating adaptor for NF-kappa B and caspase-8-dependent apoptosis. *Biochem. Biophys. Res. Commun.*, **303**, 69–73.
26. Dowds, T.A., Masumoto, J., Zhu, L., Inohara, N. and Nunez, G. (2004) Cryopyrin-induced interleukin 1beta secretion in monocytic cells: enhanced activity of disease-associated mutants and requirement for ASC. *J. Biol. Chem.*, **279**, 21924–21928.
27. Hsu, T., Trojanowska, M. and Watson, D.K. (2004) Ets proteins in biological control and cancer. *J. Cell Biochem.*, **91**, 896–903.
28. Seth, A. and Papas, T.S. (1990) The c-ets-1 proto-oncogene has oncogenic activity and is positively autoregulated. *Oncogene*, **5**, 1761–1767.
29. Topol, L.Z., Tatosyan, A.G., Ascione, R., Thompson, D.M., Blair, D.G., Kola, I. and Seth, A. (1992) C-ets-1 protooncogene expression alters the growth properties of immortalized rat fibroblasts. *Cancer Lett.*, **67**, 71–78.
30. Seth, A. and Watson, D.K. (2005) ETS transcription factors and their emerging roles in human cancer. *Eur. J. Cancer*, **41**, 2462–2478.
31. Kola, I., Brookes, S., Green, A.R., Garber, R., Tymms, M., Papas, T.S. and Seth, A. (1993) The Ets1 transcription factor is widely expressed during murine embryo development and is associated with mesodermal cells involved in morphogenetic processes such as organ formation. *Proc. Natl Acad. Sci. USA*, **90**, 7588–7592.
32. Vary, C.P., Li, V., Raouf, A., Kitching, R., Kola, I., Franceschi, C., Venanzoni, M. and Seth, A. (2000) Involvement of Ets transcription factors and targets in osteoblast differentiation and matrix mineralization. *Exp. Cell Res.*, **257**, 213–222.
33. Jayaraman, G., Srinivas, R., Duggan, C., Ferreira, E., Swaminathan, S., Somasundaram, K., Williams, J., Hauser, C., Kurkinen, M., Dhar, R. *et al.* (1999) p300/cAMP-responsive element-binding protein interactions with ets-1 and ets-2 in the transcriptional activation of the human stromelysin promoter. *J. Biol. Chem.*, **274**, 17342–17352.
34. Goldbach-Mansky, R., Dailey, N.J., Canna, S.W., Gelabert, A., Jones, J., Rubin, B.I., Kim, H.J., Brewer, C., Zalewski, C., Wiggs, E. *et al.* (2006) Neonatal-onset multisystem inflammatory disease responsive to interleukin-1beta inhibition. *N. Engl. J. Med.*, **355**, 581–592.
35. Greenhough, A., Smartt, H.J., Moore, A.E., Roberts, H.R., Williams, A.C., Paraskeva, C. and Kaidi, A. (2009) The COX-2/PGE2 pathway: key roles in the hallmarks of cancer and adaptation to the tumour microenvironment. *Carcinogenesis*, **30**, 377–386.
36. Horvath, A., Mathyakina, L., Vong, Q., Baxendale, V., Pang, A.L., Chan, W.Y. and Stratakis, C.A. (2006) Serial analysis of gene expression in adrenocortical hyperplasia caused by a germline PRKAR1A mutation. *J. Clin. Endocrinol. Metab.*, **91**, 584–596.
37. Almeida, M.Q., Muchow, M., Boikos, S., Bauer, A.J., Griffin, K.J., Tsang, K.M., Cheadle, C., Watkins, T., Wen, F., Starost, M.F. *et al.* (2010) Mouse Prkar1a haploinsufficiency leads to an increase in tumors in the Trp53+/− or Rb1+/− backgrounds and chemically induced skin papillomas by dysregulation of the cell cycle and Wnt signaling. *Hum. Mol. Genet.*, **19**, 1387–1398.
38. Iliopoulos, D., Bimpaki, E.I., Nesterova, M. and Stratakis, C.A. (2009) MicroRNA signature of primary pigmented nodular adrenocortical disease: clinical correlations and regulation of Wnt signaling. *Cancer Res.*, **69**, 3278–3282.
39. Bourdeau, I., Antonini, S.R., Lacroix, A., Kirschner, L.S., Matyakhina, L., Lorang, D., Libutti, S.K. and Stratakis, C.A. (2004) Gene array analysis of macronodular adrenal hyperplasia confirms clinical heterogeneity and identifies several candidate genes as molecular mediators. *Oncogene*, **23**, 1575–1585.
40. Bimpaki, E.I., Iliopoulos, D., Moraitis, A. and Stratakis, C.A. (2009) MicroRNA signature in massive macronodular adrenocortical disease and implications for adrenocortical tumorigenesis. *Clin. Endocrinol. (Oxf.)*, **72**, 744–751.
41. Hsiao, H.P., Kirschner, L.S., Bourdeau, I., Keil, M.F., Boikos, S.A., Verma, S., Robinson-White, A.J., Nesterova, M., Lacroix, A. and Stratakis, C.A. (2009) Clinical and genetic heterogeneity, overlap with other tumor syndromes, and atypical glucocorticoid hormone secretion in adrenocorticotropin-independent macronodular adrenal hyperplasia compared with other adrenocortical tumors. *J. Clin. Endocrinol. Metab.*, **94**, 2930–2937.
42. Skalhegg, B.S., Huang, Y., Su, T., Idzerda, R.L., McKnight, G.S. and Burton, K.A. (2002) Mutation of the Calpha subunit of PKA leads to growth retardation and sperm dysfunction. *Mol. Endocrinol.*, **16**, 630–639.
43. Wang, X., Manner, P.A., Horner, A., Shum, L., Tuan, R.S. and Nuckolls, G.H. (2004) Regulation of MMP-13 expression by RUNX2 and FGF2 in osteoarthritic cartilage. *Osteoarthritis Cartil.*, **12**, 963–973.
44. Cheadle, C., Nesterova, M., Watkins, T., Barnes, K.C., Hall, J.C., Rosen, A., Becker, K.G. and Cho-Chung, Y.S. (2008) Regulatory subunits of PKA define an axis of cellular proliferation/differentiation in ovarian cancer cells. *BMC Med. Genomics*, **1**, 43.
45. Livak, K.J. and Schmittgen, T.D. (2001) Analysis of relative gene expression data using real-time quantitative PCR and the 2(-Delta Delta C(T)) method. *Methods*, **25**, 402–408.
46. Nesterova, M., Yokozaki, H., McDuffie, E. and Cho-Chung, Y.S. (1996) Overexpression of RII beta regulatory subunit of protein kinase A in human colon carcinoma cell induces growth arrest and phenotypic changes that are abolished by site-directed mutation of RII beta. *Eur. J. Biochem.*, **235**, 486–494.
47. Neary, C.L., Nesterova, M., Cho, Y.S., Cheadle, C., Becker, K.G. and Cho-Chung, Y.S. (2004) Protein kinase A isozyme switching: eliciting differential cAMP signaling and tumor reversion. *Oncogene*, **23**, 8847–8856.
48. Rohlff, C., Clair, T. and Cho-Chung, Y.S. (1993) 8-Cl-cAMP induces truncation and down-regulation of the RI alpha subunit and up-regulation of the RII beta subunit of cAMP-dependent protein kinase leading to type II holoenzyme-dependent growth inhibition and differentiation of HL-60 leukemia cells. *J. Biol. Chem.*, **268**, 5774–5782.
49. Guerrero, M.D., Aquino, M., Bruno, I., Terencio, M.C., Paya, M., Riccio, R. and Gomez-Paloma, L. (2007) Synthesis and pharmacological evaluation of a selected library of new potential anti-inflammatory agents bearing the gamma-hydroxybutenolide scaffold: a new class of inhibitors of prostanoid production through the selective modulation of microsomal prostaglandin E synthase-1 expression. *J. Med. Chem.*, **50**, 2176–2184.
50. Molyneux, S.D., Di Grappa, M.A., Beristain, A.G., McKee, T.D., Wai, D.H., Paderova, J., Kashyap, M., Hu, P., Maiuri, T., Narala, S.R. *et al.* (2010) *Prkar1a* is an osteosarcoma tumor suppressor that defines a molecular subclass in mice. *J. Clin. Invest.*, **120**, 3310–3325.